Biochimica et Biophysica Acta 1798 (2010) 592–604

Contents lists available at ScienceDirect

Biochimica et Biophysica Acta

journal homepage: www.elsevier.com/locate/bbamem

Palmitoylation of R-Ras by human DHHC19, a palmitoyl transferase with a CaaX box

Florian Baumgart, María Corral-Escariz, Jesús Pérez-Gil, Ignacio Rodríguez-Crespo *

Departamento de Bioquímica y Biología Molecular, Facultad de Ciencias Químicas, Universidad Complutense, Madrid 28040, Spain

ARTICLE INFO

Article history:
Received 15 September 2009
Received in revised form 17 December 2009
Accepted 4 January 2010
Available online 13 January 2010

Keywords:
Palmitoyl transferases
Palmitoylation
DHHC proteins
Small GTPases
R-Ras

ABSTRACT

Mammalian proteins that contain an aspartate-histidine-histidine-cysteine-(DHHC) motif have been recently identified as a group of membrane-associated palmitoyl acyltransferases (PATs). Among the several protein substrates known to become palmitoylated by DHHC PATs are small GTPases prenylated at their carboxy-terminal end, such as H-Ras or N-Ras, eNOS, kinases myristoylated at their N-terminal end, such as Lck, and many transmembrane proteins and channels. We have focused our studies on the product of the human gene DHHC19, a putative palmitoyl transferase that, interestingly, displays a conserved CaaX box at its carboxy-terminal end. We show herein that the amino acid sequence present at the carboxy-terminus of DHHC19 is able to exclude a green fluorescent protein (GFP) reporter from the nucleus and direct it towards perinuclear regions. Transfection of full-length DHHC19 in COS7 cells reveals a perinuclear distribution, in analogy to other palmitoyl transferases, with a strong colocalization with the trans-Golgi markers Gal-T and TGN38. We have tested several small GTPases that are known to be palmitoylated as possible substrates of DHHC19. Although DHHC19 failed to increase the palmitoylation of H-Ras, N-Ras, K-Ras4A, RhoB or Rap2 it increased the palmitoylation of R-Ras approximately two-fold. The increased palmitoylation of R-Ras cotransfected with DHHC19 is accompanied by an augmented association with membranes as well as with rafts/caveolae. Finally, using both wild-type and an activated GTP bound form of R-Ras (G38V), we also show that the increased palmitoylation of R-Ras due to DHHC19 coexpression is accompanied by an enhanced viability of the transfected cells.

1. Introduction

Among post-translational modification events, protein palmitoylation is emerging as an extremely important and abundant modification of polypeptides being responsible for changes in the trafficking, activity and localization of the lipidated proteins. The identification of enzymes responsible for this covalent attachment of a 16:0 fatty acid has been elusive for many years. However, using forward genetic screens in yeast, the laboratories of R. Deschenes and M. Linder demonstrated that two *S. cerevisiae* proteins, Erf2/Erf4 are responsible for the palmitoylation of yeast Ras2 [1,2]. Sequence analysis revealed that Erf2 is very likely an integral membrane protein with 4 to 6 transmembrane domains and a hydrophilic domain containing a so-called DHHC (Asp-His-His-Cys) motive. The DHHC domain of Erf2 is necessary for the palmitoyl transferase activity, an observation that lead to the initial assumption that proteins containing this DHHC motif might be palmitoyl transferases in general. Inspection of sequence databases allowed these authors to conclude that this motif can be found not only in yeast, but also in *C. elegans*, *D. melanogaster* and mammals, comprising 23 genes containing DHHC motifs in the human genome.

In the past few years, several palmitoylated cellular proteins have been shown to be substrates for certain palmitoyl transferases of the DHHC family. Using cotransfection experiments of a putative substrate together with each of the 23 mammalian DHHC palmitoyl transferases, PSD-95 was reported to increase its palmitoylation when cotransfected with DHHC2, -3, -6, -7, -8, -10, -12, -15, -20 and -21 [3]. In partial contradiction to this report, recombinantly expressed and purified PSD-95 was reported to become efficiently palmitoylated when incubated with purified DHHC17 (also called HIP14) [4]. The fact that overexpressed DHHC17 displayed no effect on the *in vivo* palmitoylation of transfected PSD-95 clearly seems to indicate that the subcellular localization of the various palmitoyl transferases might determine which substrates are used *in vivo*. Using the same approach of overexpression of the palmitoylatable protein substrate together with each of the 23 DHHC clones allowed the identification of DHHC2, -3, -7, -8 and -21 as palmitoyl transferases of eNOS [5], DHHC3, -7, -15 and -17 for cysteine string protein [6] and DHHC3 and -7 for $G\alpha_q$, $G\alpha_S$ and $G\alpha_{i2}$ [7].

Other mammalian proteins reported to be palmitoylated by members of the DHHC family of proteins include the gamma2 subunit of the GABA receptor by DHHC3/GODZ [8], CKAP4/p63 [9] and tetraspanins CD9 and CD151 by DHHC2 [10].

Abbreviations: DHHC, Asp-His-His-Cys motif; PAT, palmitoyl acyltransferase; GFP, green fluorescent protein; HPLC, high pressure liquid chromatography; MTT, 3-(4,5-dimethylthiazol-2-yl)-2,5-diphenyltetrazoliumbromide

* Corresponding author. Departamento de Bioquímica y Biología Molecular, Facultad de Ciencias Químicas, Universidad Complutense, Ciudad Universitaria, 28040, Madrid, Spain. Tel.: +34 91 394 4137; fax: +34 91 394 4159.
E-mail address: nacho@bbm1.ucm.es (I. Rodríguez-Crespo).

0005-2736/$ – see front matter © 2010 Elsevier B.V. All rights reserved.
doi:10.1016/j.bbamem.2010.01.002

Post-translational modifications of members of the DHHC family themselves beyond the palmitate attachment during the catalytic cycle have not been reported yet. Sequence inspection of the various mammalian DHHC PATs allowed us to observe that the human isoform DHHC19 displays a CaaX box motif located at the carboxy-terminal end. With that in mind, we have undertaken the study of the catalytic properties of human DHHC19. We show herein that a synthetic peptide covering the carboxy-terminal sequence of DHHC19 is a substrate for mammalian farnesyl transferase, hence demonstrating that its CaaX box is indeed functional. This led us to investigate more carefully which substrates might become palmitoylated by DHHC19 with special focus on small GTPases of the Ras and Rho families, since many of them are known to be isoprenylated and palmitoylated. In fact, the palmitoylation of K-Ras4A [11], R-Ras [12], RhoB [13], Rap2 [14] and TC10 [15] has been observed previously. We show evidence in this manuscript that palmitoylation of R-Ras increases approximately two-fold when this small GTPase is cotransfected with DHHC19, whereas H-Ras, N-Ras, K-Ras4A, RhoB and Rap2 failed to do so. Since overexpression of DHHC19 leads to an increased palmitoylation of R-Ras accompanied by significant changes in its cellular functions our data implicate the putative palmitoyl transferase DHHC19 in the functionality of this small GTPase.

2. Materials and methods

2.1. Materials

All buffers and common laboratory reagents were obtained from Sigma (St. Louis, MO, USA) if not otherwise indicated. Using a campus facility, we obtained a rabbit polyclonal anti-GFP and anti-5′-nucleotidase antisera that were used throughout the paper. Monoclonal anti-FLAG, anti-β-COP and anti-HA antibodies were from Sigma (St. Louis, MO, USA). The rabbit polyclonal anti-caveolin1 antibody was purchased from BD Transduction Laboratories. Secondary antibodies were purchased from Sigma-Aldrich. Peptides for the *in vitro* farnesylation assay were synthesized by Thermo Scientific (Ulm, Germany). Compactin was from Merck. Fluoroguard was purchased from BioRad. Molecular Mass markers were from Fermentas.

2.2. DNA constructs

All oligonucleotides were ordered from Sigma. DHHC19wt was a generous gift from Dr. Yasuyuki Igarashi (Hokkaido University) and was cloned into pEGFP-C1 (Clontech) between BamHI and EcoRI. Full-length wild-type EGFP-H-Ras and EGFP-N-Ras were kindly provided by Dr. Mark R. Philips (NYU School of Medicine). EGFP-R-Ras, EGFP-DHHC9 and EGFP-HA-RhoB were kindly supplied by Dr. Johan Peränen (University of Helsinki), Dr. Maurine Linder (Washington University, Missouri) and Dr. Dolores López Sala (CIB Madrid), respectively. DHHC3 (also known as GODZ) was a generous gift from Dr. Masayoshi Mishima (University of Tokyo). Finally, EGFP-SNAP23 and EGFP-SNAP25 were generously provided by Dr. Luke H. Chamberlain (University of Edinburgh). All constructs corresponding to the carboxy-terminal end of H-Ras (amino acids CMSCKCVLS), N-Ras (amino acids CMGLPCVVM), R-Ras (amino acids RKKGGGCPCVLL), K-Ras4A (amino acids KTPGCVKIKKCIIM), Rap2a (amino acids DKDDPCCSACNIQ), DHHC19 (amino acids 268–282 and amino acids 258–262 of the human clone) were made using long complementary overlapping oligonucleotides that after annealing were ligated between HindIII and BamHI into pEGFP-C1 (Clontech). Likewise, complementary oligonucleotides covering the N-terminus of the Lyn kinase (amino acids MGCIKSKGKD) were designed and, after annealing, the duplex was ligated into the precut poly-linker of the pEGFP-N1 vector (Clontech) between NheI and BamHI. All internal sequence mutants were obtained using the Quick Change strategy. 3×FLAG constructs were generated by ligation of an oligo duplex containing the 3×FLAG sequence into EGFP-R-Ras that had been previously digested with NheI and BsrGI to remove the EGFP sequence. The sequences of all the clones were confirmed by automated DNA sequencing.

2.3. Recombinant expression and purification of rat farnesyl transferase

Dr. Kirill Alexandrov (Max Planck Institute of Molecular Physiology, Dortmund, Germany) kindly supplied pGATEV-FTaseα-6HisGST and pET28a-FTaseß for the recombinant expression of the rat farnesyl transferase heterodimer. In short, *E. coli* BL21 (DE3) cells were cotransformed with both plasmids. 2 l of 2X YT medium were inoculated with 20 ml of an overnight culture in the presence of 0.1 g/l ampicillin and 0.05 g/l kanamycin to maintain both plasmids. After reaching an OD of 1, protein expression was induced by the addition of 1 mM IPTG and maintained for further 20 h at 220 rpm and 30 °C. Subsequently, the cells were harvested by centrifugation in a F10 rotor (Sorvall, Norwalk, CT, USA) at 5000×*g* for 30 min and at 4 °C. Cell pellets were frozen and stored at −80 °C. Protein purification was performed in 50 mM Tris pH 7.0, 150 mM NaCl. For cell disruption a frozen cell pellet was resuspended in the presence of 0.1 g/ml CHAPS, 0.1 g/ml lysozyme and 0.01 g/ml DNAse I during 30 min on ice. After three sonication cycles of 2 min at 50% on ice, the lysate was clarified by centrifugation for 15 min at 10,000×*g* and 4 °C, filtered using a Whatman filter paper and loaded on a Ni^{2+}-NTA column (Qiagen) in the presence of 5 mM imidazole and 1 mM Mg^{2+}. After washing with several column volumes of 5 mM imidazole, the heterodimer was eluted in 200 mM imidazole. Finally, excess imidazole was removed in three extensive dialysis steps in 50 mM Tris pH 7.0 for 2 h at 4 °C.

2.4. In vitro farnesylation assay and HPLC

We followed the procedure described by Kalinin [16]. Briefly, 50 mM HEPES pH 7.2, 5 mM $MgCl_2$, 1 mM DTT, 3 mM Nonidet P40, 18 μM farnesyl pyrophosphate (if present), 50 nmol purified rat franesyl transferase and 16 nmol of the respective peptides were mixed in a reaction tube in a final volume of 500 μl and incubated at 37 °C for 30 min. Subsequently, the reaction was stopped on ice and diluted 1:1 with H_2O/0.1% TFA. In order to chromatographically resolve the modified peptides, we used a HPLC system (Beckman System Gold) and a Super Pac Pep-S 5 μm C16 reversed phase column (Pharmacia). For each sample two HPLC runs were carried out. The samples were loaded on the column in H_2O/0.1% TFA for 5 min. Then, elution was performed in a gradient of 0–70% acetonitrile during 60 min. Chromatographic profiles were recorded at either 214 nm or 280 nm depending on the presence of a tryptophan residue in the peptide sequence.

2.5. Mass spectrometry

Approximately 50 μl of the reaction mixture was passed several times through a ZipTip (Milipore) following the manufacturer's instructions and finally the peptide solution was collected. Then 1 μl was spotted onto a MALDI target plate and allowed to air-dry at room temperature. Subsequently, 0.4 μl of a 3 mg/ml of α-cyano-4-hydroxy-transcinnamic acid matrix (Sigma) in 50% acetonitrile were added to the dried peptide digest spots and allowed again to air-dry at room temperature. MALDI-TOF MS analyses were performed in a 4800 Proteomics Analyzer MALDI-TOF/TOF mass spectrometer (Applied Biosystems, Framingham, MA) at the Genomics and Proteomics Center, Complutense University of Madrid. This MALDI-TOF/TOF operated in positive reflector mode, with an accelerating voltage of 20,000 V. Mass spectra were calibrated internally using known standards. The expected peptides were selected to MS/MS sequencing analyses using the 4800 Proteomics Analyzer (Applied Biosystems, Framingham, MA). MS/MS analyses was performed with CID on (atmospheric gas was used), 1 Kv ion reflector mode and

precursor mass windows ± 5 Da. The plate model and default calibration were optimized for the MS–MS spectra processing. For protein identification, the non-redundant NCBI database (6,640,940 sequences; 2,276,975,120 amino acids) was searched using MASCOT 2.1 (matrixscience.com) through the Global Protein Server v3.6 from Applied Biosystems.

2.6. Cell culture, transfection and silencing of the DHHC19 gene using shRNAs

COS7 and NIH3T3 cells were cultivated in Dulbecco's modified Eagle's medium supplemented with 10% fetal bovine serum (Cambrex) in a humidified atmosphere containing 5% CO_2. For the experiments the cells were seeded in 6-well or 24-well plates and transfected with Escort IV (Sigma) following the supplier's instructions. One to two micrograms of DNA was used for transfection of one well of a 6-well plate. Transfections in 24-well plates were scaled down accordingly.

Silencing of the DHHC19 gene was performed using shRNAs purchased from Sigma-Aldrich. The purchased plasmids are derived from the pLKO vector. They are referenced to gene NM_144637 zinc finger, DHHC-type containing isoform 19. The sequences used are outlined below:

TRCN0000138832 NM_144637.2-301s1c1
CCGGGTTATCACAGGCTCCCTCTTTCTCGAGAAAGAGGGAGCCTGTG
ATAACTTTTTTG
TRCN0000138529 NM_144637.2-314s1c1
CCGGCCCTCTTTGTCCTTACCTTCTCTCGAGAGAAGGTAAGGACAAA
GAGGGTTTTTTG
TRCN0000137344 NM_144637.2-540s1c1
CCGGCAAGTGGGTCAATAACTGCATCTCGAGATGCAGTTATTGACCC
ACTTGTTTTTTG
TRCN0000134852 NM_144637.2-325s1c1
CCGGCTTACCTTCTTCAGTCTTGTTCTCGAGAACAAGACTGAAGAAGG
TAAGTTTTTTG
TRCN0000134807 NM_144637.2-845s1c1
CCGGCCAGCAACTGGTATTTAACAACTCGAGTTGTTAAATACCAGTT
GCTGGTTTTTTG

Transfection of COS7 cells with the silencing plasmids was performed 36 h before labelling of R-Ras with tritiated palmitic acid. We used a control consisting of empty pLKO plasmid (also available from Sigma-Aldrich).

2.7. Coimmunoprecipitation of R-Ras and its active V38 mutant with DHHC19

COS7 cells were transfected with 3×FLAG-tegged full-length R-Ras or its constitutively active V38 mutant in the absence or presence of GFP-tagged wild-type full-length DHHC19. Cells were lysed in RIPA buffer at 4 °C. The cellular debris was removed after centrifugation at 3000×*g* in a refrigerated table-top microcentrifuge. The soluble fraction was incubated with 10 µg of polyclonal rabbit anti-GFP antiserum overnight at 4 °C and finally 25 µl of a protein-A (Sigma-Aldrich) beads suspension was added to the samples. The cell lysates were centrifuged at 15,000×*g* in a table-top refrigerated centrifuge for 10 min and the supernatants were removed. The beads were washed extensively with RIPA buffer and the amount of R-Ras that was coimmunprecipitated with GFP-tagged DHHC19 was determined using anti-FLAG antibodies. An input control is shown that reflects the amount of wild-type or V38 R-Ras in the initial lysates.

2.8. Metabolic labelling with [^{3}H]-palmitic acid

For assessment of [^{3}H]-palmitate incorporation, COS7 cells ~20 h post-transfection were pre-incubated with serum free Dulbecco's modified Eagle's medium supplemented with delipidized BSA (10 mg/ml) for 1 h. Subsequently, 250 µCi/ml [^{3}H]-palmitate (first dried, then resuspended in 10 µl DMSO and diluted in an appropriate amount of medium with 10 mg/ml delipidized BSA) were added and the cells were incubated for 5 h at 37 °C. Then the cells were harvested, lysed in RIPA lysis buffer and 3× SDS application buffer containing DTT at a final concentration of 10 mM was added. Finally the samples were boiled for no more than 2 min (to avoid thioester bond hydrolysis) and resolved by SDS PAGE. The gels were fixed and soaked in Amplify reagent (GE Healthcare) for 20 min. Then they were vacuum-dried and examined by autoradiography. Duplicate gels were prepared for Western blotting.

2.9. Metabolic labelling with [^{14}C]-mevalonic acid

COS-7 cells were seeded 24 h prior to transfection in 24-well plates, and transfected using Escort IV transfection reagent. About 24 h post-transfection cells were pre-incubated with 50 µM compactin in DMEM/10% FBS for 3 h. Meanwhile, 25 µCi [^{14}C]-mevalonic acid lactone (provided in ethanol) was dried, resuspended first in 5 µl DMSO and then in DMEM/10% FBS supplemented with 50 µM compactin yielding a final concentration of 30 µCi/ml. Cells were incubated for 20 h in the presence of [^{14}C]-mevalonic acid before processing for SDS PAGE, Western blotting and autoradiography as described for metabolic labelling with [^{3}H]-palmitic acid.

2.10. Sample preparation for gel electrophoresis

Generally, samples were prepared in 3× SDS sample buffer supplemented with a final concentration of 5% β-mercaptoethanol and boiled for 5 min at 95 °C (except for samples from metabolic labelling experiments). In the case of DHHC19 it was necessary to avoid boiling the samples for immunodetection in Western blotting. Therefore, samples for immunodetection of DHHC proteins were incubated at 37 °C for 30 min prior to electrophoresis. Immunoblots were developed using ECL and a LAS3000 Imaging system from Fuji.

2.11. Enrichment of low-density membrane fractions

Low density caveolin/lipid raft containing fractions were enriched in a discontinuous sucrose gradient essentially as described previously, following our modifications to Lisanti's original reference [17,18]. Briefly, an appropriate amount of transiently transfected COS7 cells (typically four F-75 flasks) was lysed in MES buffered saline (MBS) (25 mM MES pH 6.5, 0.15 M NaCl) by 30 0.5×16 mm syringe strokes on ice. Subsequently, 1% Triton X-100 (final concentration in the lysis volume) was added and the samples were incubated for 30 min on ice. If a smaller amount of transfected cells was used, the percentage of Triton X-100 was scaled down proportionally. After a short centrifugation of 5 min at 1500×*g* and 4 °C, the supernatants were mixed with an 80% sucrose solution in MBS and placed in the bottom of the tubes. Then the rest of the 40–30–5% discontinuous sucrose gradient was formed and centrifuged for 16 h at 100,000×*g* and 4 °C in a SW65 rotor (Beckman). Next day, fractions of 400 µl were collected from the bottom of the tubes and precipitated by adding 500 µl ice cold acetone for at least 2 h. The precipitates were obtained by centrifugation for 10 min at 16, 000×*g* at 4 °C. The samples were then dried in a Univap for 10 min and prepared for SDS PAGE by the addition of 75 µl application buffer with 5% β-mercaptoethanol.

2.12. MTT viability assay

To assess the viability of cells in the presence of R-Ras with or without cotransfected DHHC19, we quantified the reduction of 3-(4,5-dimethylthiazol-2-yl)-2,5-diphenyltetrazoliumbromide (MTT) to its formazan salt as previously described [19]. Briefly, NIH 3T3 cells were

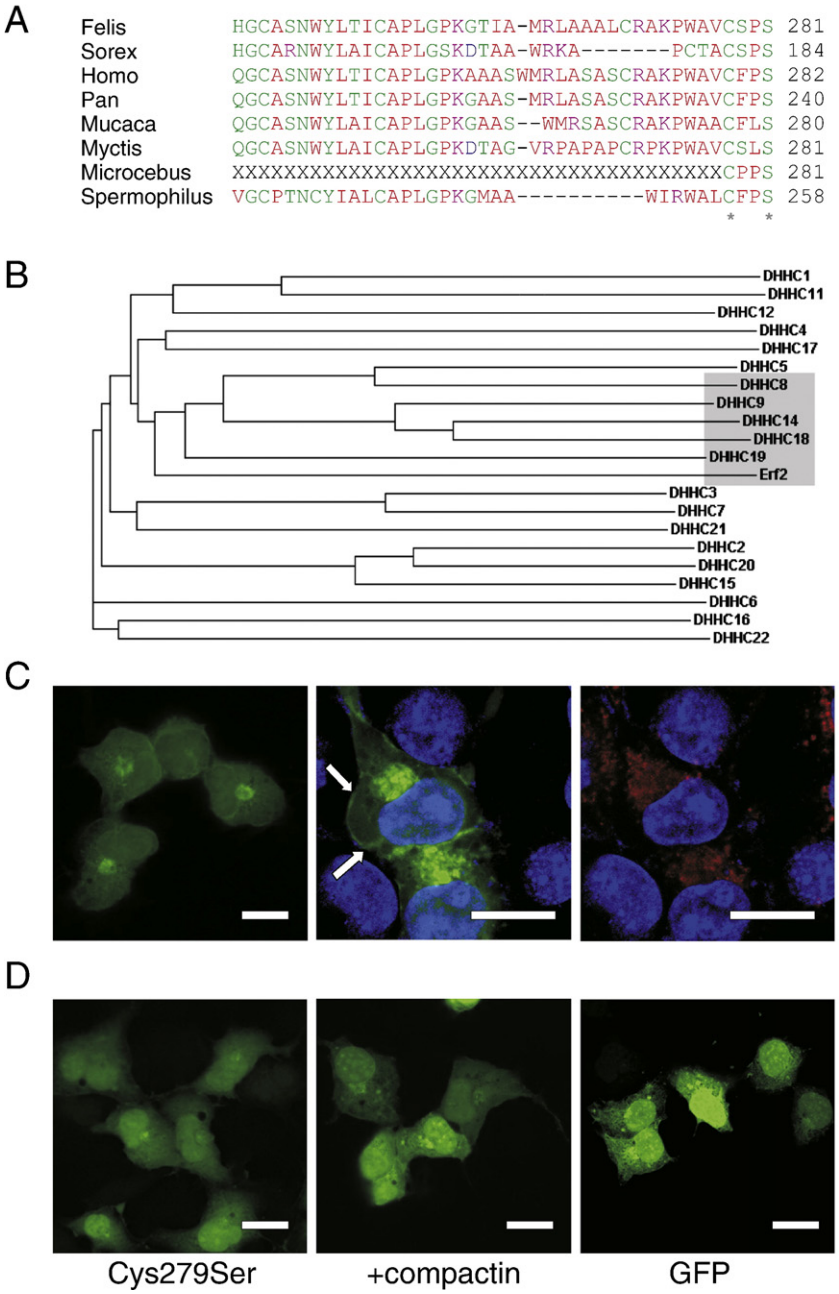

Fig. 1. Phylogenetic analysis of the carboxy-terminal end of DHHC19 and subcellular localization when transfected in COS7 cells. (A) The carboxy-terminal sequences of DHHC19 proteins were aligned and compared among various mammals. The accession number for the human isoform is AAH22078. The conserved Cys residue present in the CaaX box as well as the final Ser residue is marked with an asterisk. The presence of this Ser residue very likely determines that the protein should become farnesylated rather than geranylgeranylated [38]. (B) Phylogenetic comparison of members of the human DHHC family together with their yeast ortholog Erf2. Proteins of this family which have been reported to increase the palmitoylation of H-Ras include DHHC18 [3] and DHHC9 [20]. All these DHHC proteins are in the same branch as DHHC19 (shaded area). The sequence comparison and the phylogenetic analysis were performed using the Clustal W2 program. (C) Amino acids 258–282 of human DHHC19 were fused in frame to GFP and COS7 cells were transfected with this construct. A clear enrichment in perinuclear areas (left and middle panel) that display a certain colocalization with the Golgi marker ß-COP (labelled in red) can be observed. A small fraction of the GFP-tagged DHHC19 displays plasma membrane localization (middle panel, arrows). Cell nuclei are stained with Hoechst and are depicted in blue. (D) Mutant C279S of DHHC19 (amino acids 258–282) fused to GFP displays a clear nuclear and cytosolic staining characteristic of untagged GFP (left panel). A similar phenotype can be observed when COS7 cells transfected with the wt version were incubated with 50 µM compactin for 20 h (middle panel). The right panel shows the distribution of untagged GFP transfected in COS7 cells for comparison. Bars, 50 µM.

seeded in a 24 well plate at 100,000 cells/well and transfected the following day. About 24 h post-transfection the medium was changed to FBS-free DMEM. After another 48 h the medium was removed and the cells were incubated for ~4 h in DMEM supplemented with 0.5 mg/ml MTT. Finally, the medium was removed and the precipitated salt was dissolved in a 0.04 N HCl/isopropanol solution for quantification at 570 nm.

3. Results

3.1. DHHC19 contains a functional CaaX box at its C-terminus

Sequence comparison between the carboxy-terminal end of the product of the human gene DHHC19 and some of its mammalian orthologs revealed that the CaaX box is conserved among several

species (Fig. 1A). It is noteworthy that this motif is present in DHHC19 genes from humans, chimps, macaques and small mammals (cat, shrew, lemur, etc.) but it is absent from DHHC19 of murine genomes. In addition, a Cys residue upstream the CaaX box can be observed in most of the cases, a fact that is indicative of the carboxy-terminus of DHHC19 being probably prenylated and palmitoylated. In addition, phylogenetic analysis of DHHC genes together with the yeast homolog Erf2 showed that the DHHC19 gene is evolutionarily related to Erf2, a gene known to be involved in the palmitoylation of purified H-Ras and N-Ras *in vitro*, two small GTPases that also display CaaX boxes [20] (Fig. 1B).

In order to ascertain if the CaaX box of DHHC19 is functional inside mammalian cells we decided to fuse the final 25 amino acids of this putative palmitoyl transferase to the GFP reporter. Transfection of COS7 cells with this construct resulted in a clear perinuclear staining and a partial membrane labelling (Fig. 1C). The perinuclear distribution displays a certain colocalization with the Golgi marker ß-COP (Fig. 1C; red). When we mutated the Cys amino acid present in the CaaX box and replaced it with a Ser (C279S) the distribution was clearly altered and the cells displayed a GFP fluorescence that was indistinguishable from that of the GFP reporter alone (staining of the cytoplasm and nucleus) (Fig. 1D). Likewise, when the cells were treated with the statin compactin for 20 h, thereby altering the normal synthesis of farnesyl pyrophosphate, the fluorescence also reverted to that of GFP alone. Taken together, our data indicate that the CaaX box of DHHC19 is functional at least when fused to a GFP reporter and analyzed in transfected cells.

We next decided to inspect if a synthetic peptide corresponding to the carboxy-terminal 20 amino acids of human DHHC19 could be a substrate for recombinant farnesyl transferase. We expressed and purified to homogeneity the farnesyl transferase heterodimer (Fig. 2A) and tested if it could use peptides that display a CaaX box as substrates. As a positive control we used a peptide corresponding to the final 20 amino acids of H-Ras (Fig. 2B). Additionally, reaction in the absence of farnesyl pyrophosphate was prepared in parallel as a negative control. When we analyzed the HPLC elution profile of the H-Ras peptide at 214 nm in the absence (Fig. 2B, upper panel) or in the presence (Fig. 2B, bottom panel) of farnesyl pyrophosphate a novel peak that eluted at 49 min could be observed in the latter (marked with an asterisk). While the unmodified peptide eluted at 28 min approximately (marked with an arrow), the novel peak appeared at 49 min only when farnesyl pyrophosphate was present. This peak was assigned to the farnesylated form of H-Ras, since it eluted in the more hydrophobic fractions and its appearance was concomitant with a decrease in the concentration of the unmodified peptide. Likewise, we tested if the carboxy-terminal peptide corresponding to human DHHC19 could also be a substrate of prenyl transferase. The unmodified peptide eluted at 33.5 min approximately and could be also detected at 280 nm due to the presence of a tryptophan amino acid in its sequence (Fig. 2C, marked with an arrow). In the presence of farnesyl pyrophosphate a new peak appeared at 52 min (Fig. 2C, bottom panel, asterisk). This peak was assigned to the farnesylated form of the DHHC19 peptide (see below). In addition, we also analyzed the mixture by mass spectrometry techniques (Fig. 2E). The MS spectrum displayed the presence of the unmodified peptide at the expected molecular mass of 1609.90 Da whereas the modified peptide appeared at 1813.97 Da. This molecular mass difference of 204 Da is in agreement with the mass expected with a farnesyl moiety being attached to the Cys residue within the CaaX box present in the peptide. MS/MS analysis allowed us to unequivocally identify the amino acid sequence and the modified Cys residue, both in the y and in the b series (Fig. 2E). In addition, we assessed incorporation of the isoprene moiety labelling cells with its precursor [^{14}C]-mevalonic acid in COS-7 cells that overexpress GFP-DHHC19 (Fig. 2D). As a positive control we used GFP-H-Ras. A mutant version of DHHC19 in which the reactive cysteine of the CaaX box was mutated to serine (C279S) was also used. While we managed to detect the incorporation of the radiolabelled isoprene into H-Ras, labelling of DHHC19 was not detected. This indicates that detection of DHHC19 is below our detection limit at the observed expression levels. Unfortunately, under our assay conditions we were not able to obtain expression levels of DHHC19 that were comparable to those of H-Ras (Fig. 2D bottom panel).

3.2. Subcellular distribution of DHHC19

The subcellular distribution of human full-length DHHC19 was inspected by fusing the gene to the carboxy-terminal end of GFP and subsequent transfection of the plasmid in COS7 cells. DHHC19 localized predominantly to the perinuclear regions of the cell (Fig. 3A). When we compared this staining with that of the Golgi marker ß-COP or with the two different trans-Golgi-network markers Gal-T and TGN38 we could observe an almost complete overlap in the latter cases. Hence, DHHC19 localizes predominantly to the trans-Golgi-network, probably regulating from this site the proper palmitoylation of proteins that proceed along intracellular sorting pathways. Unlike the distribution shown by the final 25 amino acids of DHHC19 fused to GFP, no plasma membrane staining could be observed in the case of the full-length protein. Inspection of the human DHHC19 sequence reveals the existence of four putative transmembrane helices flanking the ~50 amino acids DHHC motif, on each side [21]. In order to analyze if the CaaX box positioned at the carboxy-terminus of DHHC19 dictated a certain subcellular distribution, we mutated Cys279 and analyzed the phenotype of the full-length C279S DHHC19 mutant when fused to the GFP reporter (Fig. 3B). Unlike the phenotype displayed by the final 25-amino acid stretch of DHHC19 when fused to GFP (Fig. 1C and D), mutation of Cys 279 within a full-length context did not render a significant change in the subcellular localization when compared with the wild-type protein. This led us to conclude that the subcellular localization is mostly dictated by the transmembrane helices or by other structural motifs in the global fold of the protein. It is also conceivable that *in vivo* the CaaX box of DHHC19 might be responsible for the preferential localization in membranes with a certain lipid composition.

With all this in mind we performed sucrose density gradient centrifugations in order to analyze how the various DHHC19 constructs behaved in terms of association with raft/caveolae membrane fractions. We used two controls of proteins associated with detergent-resistant fractions: the GPI-anchored 5′-nucleotidase and caveolin-1 (Fig. 4). These proteins were predominantly enriched in the fractions 6–8 (1 being the bottom and 10 the top of

Fig. 2. The carboxy-termini of both H-Ras and human DHHC19 are substrates for purified farnesyl transferase. (A) Plasmids encoding the α and β subunits of mammalian farnesyl transferase were cotransformed in *E. coli* and after recombinant expression, the heterodimeric farnesyl transferase was purified using a Ni^{2+}-NTA affinity resin. The purity of the eluted sample was analyzed by SDS PAGE and Coomassie staining. (B) HPLC analysis of a human H-Ras peptide comprising the final 15 amino acids incubated in the absence (upper panel) or presence (bottom panel) of farnesyl pyrophosphate. The reaction was allowed to proceed for 20 min at 37 °C before injection into the HPLC column. Separation was performed using a C16 reversed phase column and an acetonitrile gradient (0–70% in 60 min) as described in the Section 2 . The arrows indicate the elution position of the unmodified peptide, whereas the asterisk denotes the position of the prenylated peptide. The elution profile was obtained at 214 nm. (C) Likewise, a peptide corresponding to the carboxy-terminal 15 amino acids of DHHC19 was tested as a substrate for recombinant, purified prenyl transferase. Elution was monitored at 280 nm and the conditions were as stated above. Similar results were obtained in three independent runs. (D) In order to assess the isoprenylation of DHHC19 *in vivo*, we carried out metabolic labelling with its precursor [^{14}C]-mevalonic acid in COS-7 cells overexpressing either GFP-DHHC19 or the CaaX box mutant SaaX (DHHC19 C279S) or GFP-H-Ras as controls. The bottom panel is a blotting against GFP-tagged H-Ras, GFP-tagged-DHHC19 as well as its non-prenylated mutant Cys279Ser. The upper panel is the corresponding autoradiogram. No isoprenoid incorporation could be detected under our assay conditions. (E) MALDI TOF/TOF fragmentation of the product of the reaction of purified mammalian prenyl transferase on the DHHC19 peptide and de novo sequencing revealing the presence of the prenylated Cys within the CAAX box. The y and b series are depicted on top.

the gradient). On the other hand, both ß-COP (a membrane-associated protein that excludes from rafts/caveolae) and untagged GFP appear mostly in the bottom fractions, that is, fractions 1–3 (Fig. 4). When we analyzed the flotation behaviour of the chimeras comprising 15 (amino acids 268–282) or 25 (amino acids 258–282) amino acids of the carboxy-terminus of DHHC19 fused to GFP we could observe that enriched they reached the low-density fractions to a limited extent. Likewise, the short DHHC19 chimera with the

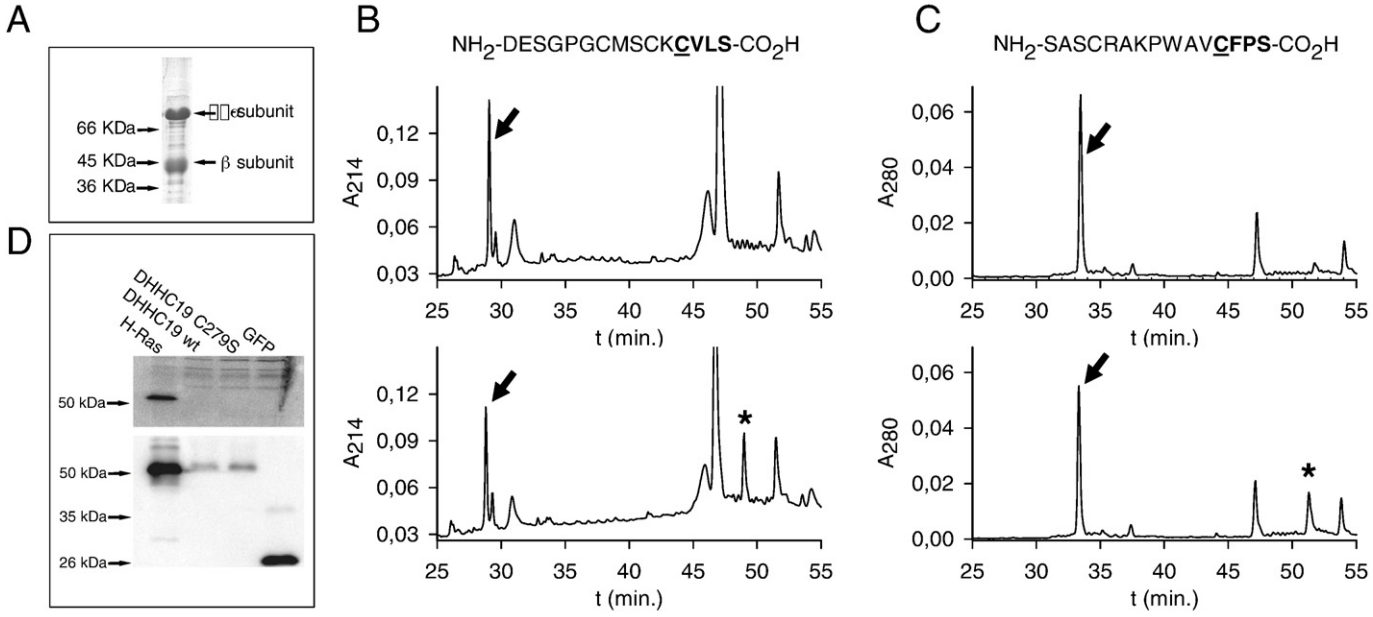

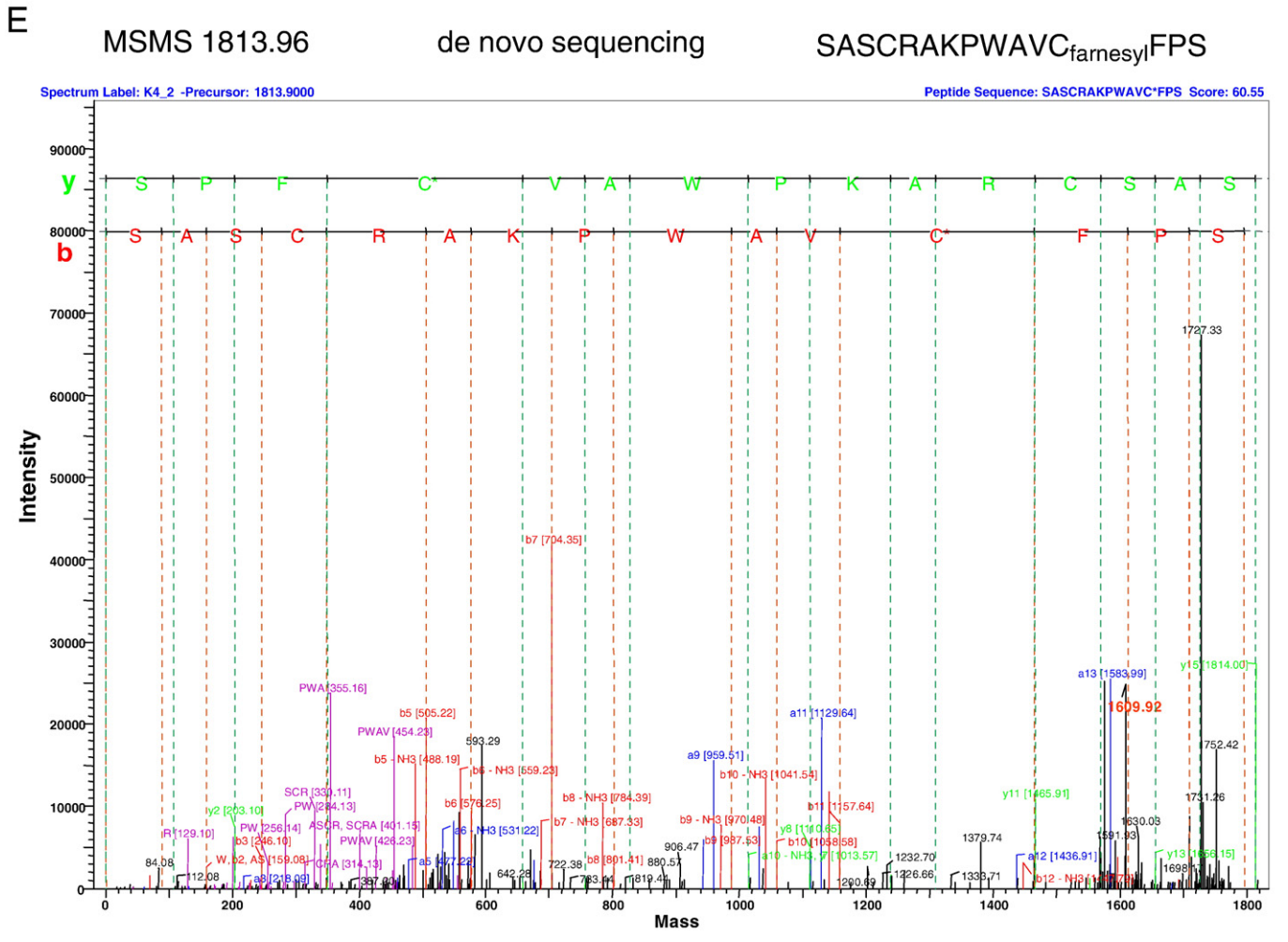

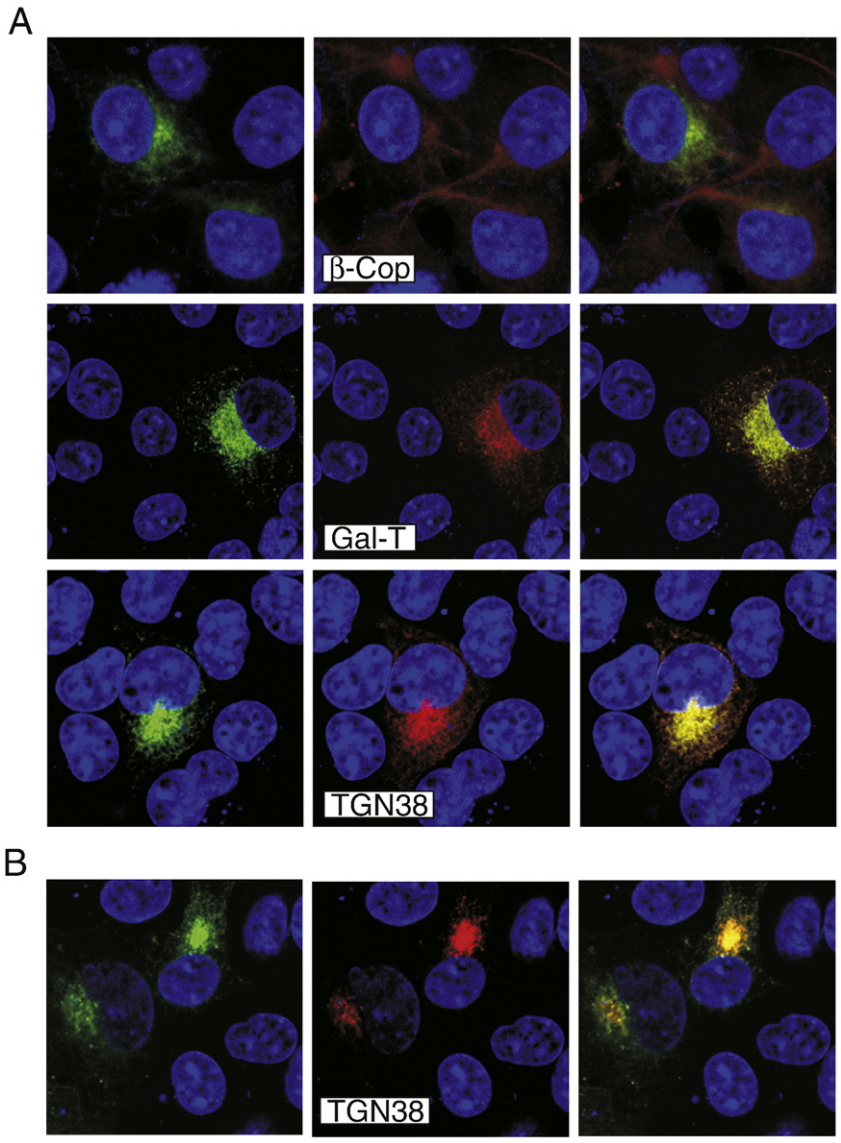

Fig. 3. GFP-tagged DHHC19 displays a perinuclear localization. (A) COS7 cells were transfected with a GFP-tagged chimera of full-length DHHC19 and its subcellular distribution was analyzed by laser confocal microscopy comparing it to three other proteins. The left column shows the distribution of DHHC19, the middle column the distribution of ß-COP, Gal-T or TGN38 and the right column is the merge column. Antibodies against ß-COP, a cis-, medium-Golgi marker were added to the permeabilized cells and a Cy3 secondary antibody was added to reveal its distribution. Alternatively, COS7 cells were cotransfected with the plasmids encoding for the trans-Golgi-network markers Gal-T or TGN38 fused to CFP. Double positive cells are shown. For clarity, the CFP signal is shown in red. (B) Equally, COS7 cells were transfected with a mutant of full-length DHHC19 in which the Cys residue that becomes prenylated had been substituted for Ser (C279S) and its colocalization with TGN38 was analyzed by laser confocal microscopy.

eliminated CaaX box (C279S) was mostly localized to the bottom fractions and in this case, no colocalization with caveolin-1-enriched fractions could be observed. We also cloned as controls the final 11 amino acids of human H-Ras and N-Ras in frame with GFP and analyzed to which degree they were able to become enriched in lipid rafts/caveolae. As shown in Fig. 4, these two constructs appeared in fractions 1–6 and their colocalization with caveolin-1 was very limited, even considering the fact that N-Ras is supposed to be prenylated and partially monopalmitoylated and H-Ras prenylated and partially dipalmitoylated. Consequently, the rafts/caveolae enrichment of all these short prenylated constructs seems to be very limited.

Conversely, both full-length wild-type DHHC19 and its non-prenylated counterpart, both of which presumably have four trans-membrane helices, localized partially to rafts/caveolae (Fig. 4). Thus, this DHHC isoform seems to be, albeit partially, capable to become enriched in the detergent-resistant fractions, in analogy to isoforms DHHC2, -3, -7, -8 and -21 [5]. Interestingly, the prenylated and dually palmitoylated full-length H-Ras displayed a clear partial localization in raft/caveolae, whereas full-length N-Ras did so to a lesser extent.

3.3. Substrate specificity of DHHC19

A tempting idea would be that the prenylation of DHHC19 conveys substrate specificity for prenylated substrates. Therefore, we started our search for putative substrates of DHHC19 with H-Ras since its palmitoylation at Cys amino acids 181 and 184 is well established [22]. COS7 cells were transfected with GFP-tagged full-length H-Ras (Fig. 5, left panel) or GFP fused to the final 11 amino acids of H-Ras (that include the prenylation and palmitoylation sites) (Fig. 5, right panel). Cells were also cotransfected with various DHHC19 constructs and we inspected the amount of palmitoylated H-Ras that could be detected by metabolic labelling. When COS7 cells were incubated with tritiated palmitic acid a clear palmitoylated band could be observed at the corresponding molecular mass in the absence of any transfected DHHC19 isoform both for the long and short GFP-tagged

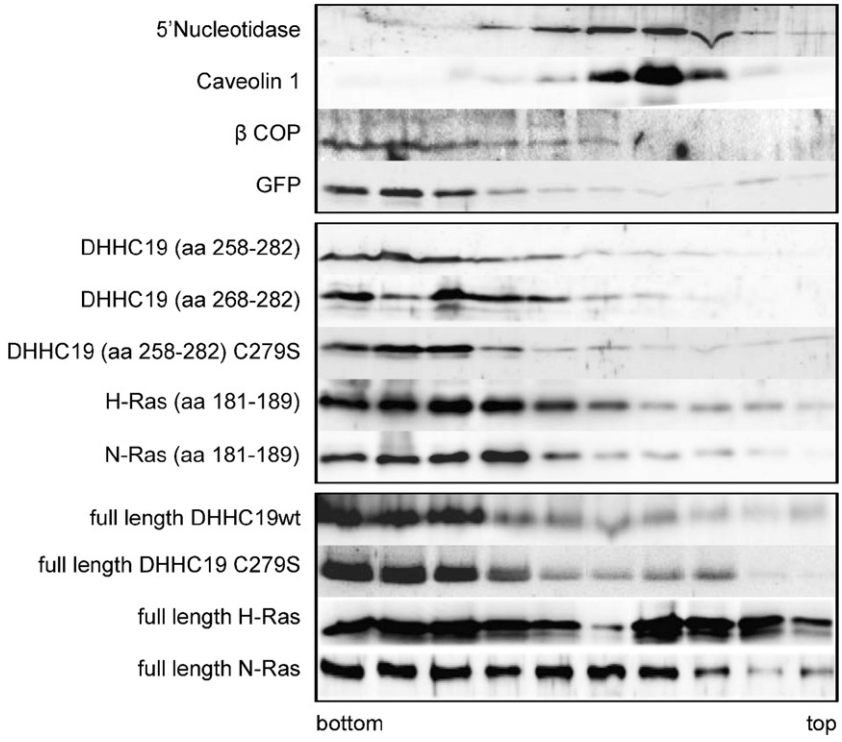

Fig. 4. Full-length DHHC19 is only marginally associated with rafts/caveolae. Sucrose gradient analysis of various constructs transfected in COS7 cells. We used 5′-nucleotidase (a GPI-anchored protein) and caveolin-1 as markers for rafts/caveolae and their localization was determined using specific antibodies. Both GFP and the membrane-associated protein ß-COP appeared in the bottom fractions. In the middle panel, short constructs of the carboxy-terminal end of DHHC19 fused to GFP are shown. Short constructs of N-Ras and H-Ras under identical conditions are shown for comparison. In the bottom panel, the flotation pattern of GFP-tagged full-length constructs of DHHC19, a non-prenylated mutant C279S, N-Ras and H-Ras are also depicted. In the two bottom panels GFP-tagged chimeras were used and the localization of the proteins was determined using anti-GFP antibodies. Results are representative of three independent flotation experiments.

constructs of H-Ras. This result indicates that one or several of the palmitoyl transferases present in COS7 cells can use H-Ras as a substrate. Unfortunately, we were unable to observe any increase in the degree of palmitoylation when cells were cotransfected with wild-type DHHC19, a mutant in which the DHHC motif had been converted into DHHG, a non-prenylated form of DHHC19 or a non-catalytic chimera in which the final 25 amino acids of DHHC19 had been fused to GFP (Fig. 5). Consequently, we concluded that DHHC19 does not display any palmitoyl transferase activity towards H-Ras.

Next, we inspected if overexpression of DHHC19 in COS7 cells could increase palmitoylation of some cotransfected substrates (Fig. 6A). This time we used DHHC9 as a control, since DHHC9 has been reported to be

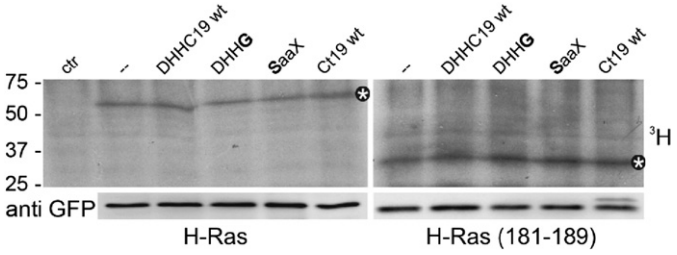

Fig. 5. Human H-Ras is not a substrate for DHHC19. COS7 cells were transfected with GFP-tagged full-length H-Ras (left panel) or the GFP-tagged C-terminal region of H-Ras (aa 181–189) (right panel). The symbol "—" means that in that well no DHHC plasmid was cotransfected with H-Ras whereas GFP was transfected in the control lane. Labelling with [^{3}H]-palmitic acid was performed as described in the Section 2. The gels were dried and palmitic incorporation was assessed by film exposure after 1 week. Cells were cotransfected with either wild-type DHHC19 or mutants DHHG or SaaX (in which the CaaX box of DHHC19 CFPS had been converted into SFPS). In addition, COS7 cells were also cotransfected with a construct in which amino acids 258–282 of DHHC19 (that is, the carboxy-terminal end) had been fused to the GFP reporter. The amount of GFP-tagged H-Ras loaded was confirmed by Western blot (bottom). Asterisks denote the position of bands corresponding to the labelled transfected proteins in either case.

a palmitoyl transferase for both H-Ras and N-Ras *in vitro*. When H-Ras, N-Ras and DHHC9 together with its proposed co-factor GCP16 were expressed and purified from a baculovirus system, incubation of the palmitoyl transferase plus GCP16 with either of the two small GTPases resulted in increased palmitoylation [20]. However, no studies have been reported to date in which this result could be corroborated *in vivo*. We tested small GTPases with palmitoylatable Cys amino acids that were located close to the prenylated Cys residue present in the CaaX box (see sequences in Fig. 6A). In our hands, neither DHHC9 nor DHHC19 were able to result in a clear increased palmitoylation of the small GTPases H-Ras, N-Ras, RhoB, Rap2 or K-Ras4A (Fig. 6A). Since GCP16 is ubiquitously expressed, it was not necessary to transfect it as well [21]. Nevertheless, DHHC19 was able to induce a two-fold increase in the palmitoylation of R-Ras. This increase is similar to that reported for eNOS in the presence of DHHC21 (three-fold in this case), which is the palmitoyl transferase that regulates its palmitoylation in the endothelium [5] or for PSD95 in the presence of DHHC2 (2.8-fold) or DHHC3 (2.4-fold) [3]. The position of the transfected DHHC19 and DHHC9 PATs obtained in all these substrate labelling experiments is shown on the bottom right panel of Fig. 6A.

We are well aware of the fact that the complete ineffectiveness of DHHC9 as a palmitoyl transferase when confronted with H-Ras and N-Ras as substrates is somehow in contradiction with previous results [20]. However, it is possible that the published palmitoylation of H-Ras and N-Ras by DHHC9 can be observed only *in vitro*, when the recombinant purified proteins are incubated together but not *in vivo* inside the cell. This could also be a possible explanation for previous apparently contradictory data [4].

Since prenylation of a certain protein substrate did not seem to be a general requirement for substrate recognition by DHHC19, we also tested three additional protein substrates: the myristoylated and palmitoylated Lyn kinase, for which no DHHC palmitoyl transferase has been identified yet, as well as SNAP25 and SNAP23 for which

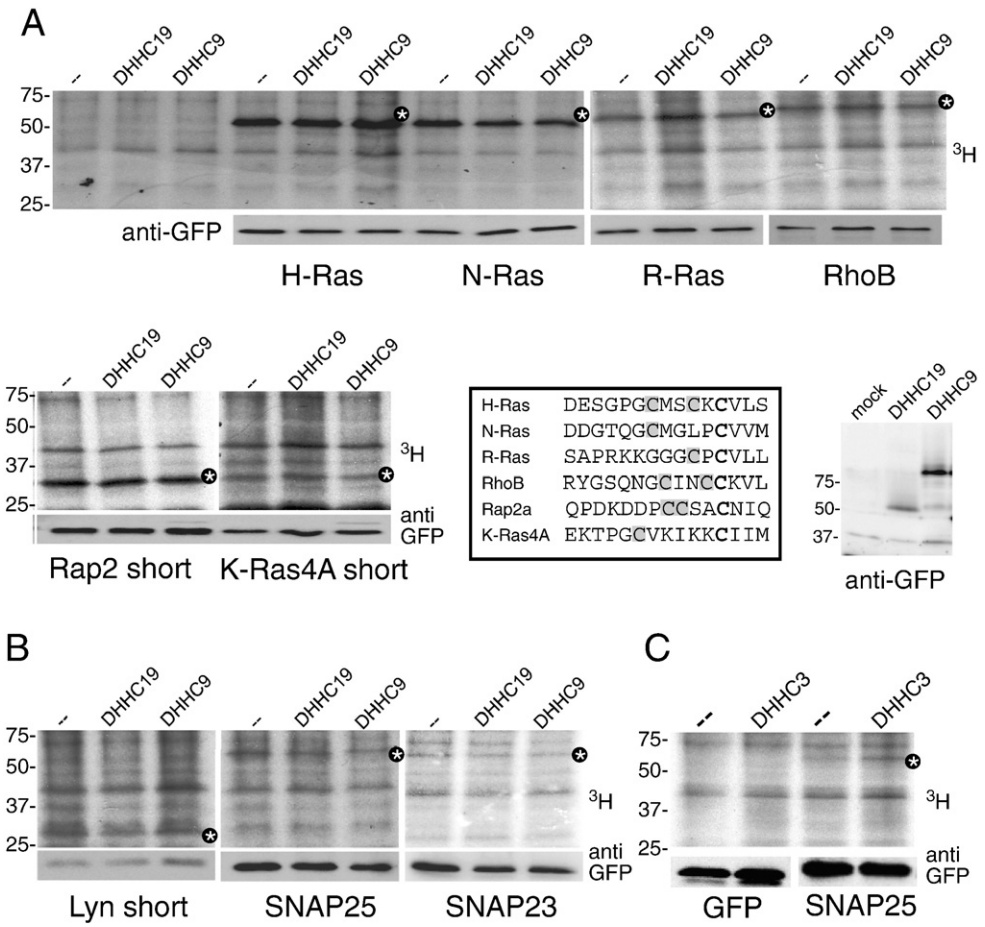

Fig. 6. Identification of R-Ras as a substrate for DHHC19. (A) Among various palmitoylated small GTPases, R-Ras is the only substrate of DHHC19. COS7 cells were transfected with plasmids encoding for six small GTPases known to be palmitoylated: H-Ras, N-Ras, R-Ras, RhoB, Rap2 and K-Ras4A. All of them were GFP-tagged and the first four of them correspond to full-length proteins. Conversely, Rap2 and K-Ras4A were chimeras of GFP fused to their carboxy-terminal 11 amino acids, which include the palmitoylation sites. Loading controls are shown at the bottom of each gel. The position of the band corresponding to the palmitoylated transfected protein is marked with an asterisk. Each of the six substrate proteins was cotransfected with an empty plasmid, with DHHC19 or with DHHC9. The amino acid sequences corresponding to the carboxy-terminal ends of the six small GTPases tested are also shown (box). The Cys residue of the CaaX box is in bold whereas the palmitoylatable Cys amino acids are shaded. Representative immunodetection of the GFP-tagged transfected DHHC19 and DHHC9 palmitoyl transferases in COS7 cells is shown (right panel). (B) In addition, three other non-isoprenylated substrates were tested. The N-terminal 10 amino acids of the kinase Lyn were fused to the GFP reporter, transfected in COS7 cells and tested in order to inspect if the degree of palmitoylation is increased in the presence of DHHC19 or DHHC9 (left panel). Likewise, GFP-tagged full-length SNAP23 and SNAP25 were also tested in the presence of these two palmitoyl transferases. The position of the band corresponding to the palmitoylated transfected protein is marked with an asterisk. (C) As a control for our assay conditions, we cotransfected GFP-tagged full-length SNAP25 with DHHC3 (GODZ), a previously published PAT-substrate pair. Palmitate incorporation increased considerably in the presence of GODZ. Results are representative of three independent experiments.

DHHC3, DHHC7 and DHHC17 have shown palmitoyl transferase activity [3,4]. In all three cases, the proteins were fused to the GFP reporter. In the case of Lyn kinase, just the 11 amino-terminal amino acids were fused, whereas in the case of SNAP25 and SNAP23, the full-length proteins were tested. As shown in Fig. 6B, neither DHHC9 nor DHHC19 were able to increase the palmitoylation levels of the product of these three genes when transfected in COS7 cells. However, cotransfection of SNAP25 with DHHC3 resulted in a very significant increase in the degree of palmitoylation (over three-fold).

3.4. DHHC19 is a major PAT towards R-Ras

Since R-Ras was the only small GTPase for which DHHC19 displayed PAT activity, we focused on the physiological effects that its hyperpalmitoylation might produce. First, we wanted to make sure that the effect on R-Ras was not perturbed by the bulky GFP tag. As shown in Fig. 7A, cotransfection of COS7 cells with DHHC19, but not with GFP or DHHC9, also increases 3×FLAG-R-Ras palmitoylation ~1.8-fold. Likewise, the DHHC19 C142G mutant, in which the catalytic motif is converted into DHHG, failed to increase 3×FLAG-R-Ras palmitoylation when compared with its wild-type counterpart (Fig. 7B). Next we decided to knock down the endogenous DHHC19 levels present in COS-7 cells using shRNA targeted against this gene. We used five different commercially available shRNA specifically designed against the DHHC19 gene (NM_144637) and tested the palmitoylation levels of transfected full-length R-Ras. As shown in Fig. 7C, all the transfected shRNA were able to diminish, albeit to a different degree, the palmitoylation of R-Ras in COS-7 cells. In fact, shRNA529, shRNA344 and shRNA344 lowered R-Ras palmitoylation levels to approximately 50% of those found in untreated cells. The fact that some R-Ras palmitoylation remains even in the presence of the various shRNAs might well indicate that other cellular DHHC isoforms might be also active towards R-Ras within COS-7 cells.

3.5. Hyperpalmitoylation of R-Ras by DHHC19 modulates its interaction with membranes

The increased palmitoylation of R-Ras caused by DHHC19 coexpression in COS7 cells resulted in a clear shift in the supernatant:pellet ratio of R-Ras distribution when cell fractionation was performed (Fig. 8A). GFP-R-Ras transfected in COS7 cells and fractionated at

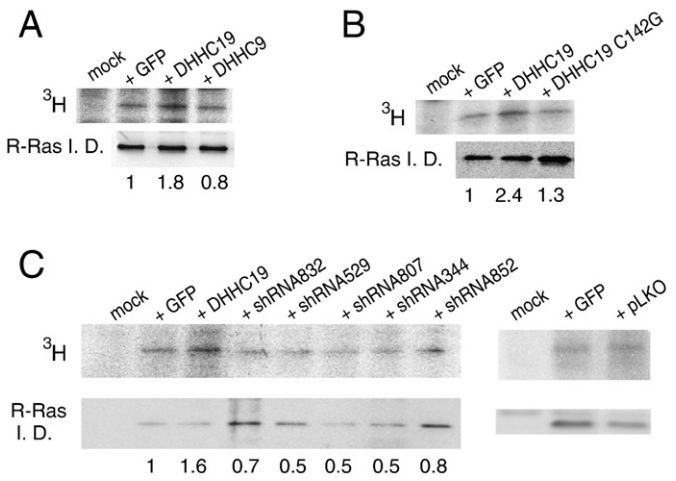

Fig. 7. Characterization of DHHC19 PAT activity towards R-Ras. (A) Palmitoylation of 3×FLAG-tagged R-Ras also shows moderate, but stable increase in the presence of GFP-DHHC19 but not in the presence of GFP or GFP-DHHC9 in COS-7 cells. Immunodetection was carried out with a monoclonal anti-FLAG antibody. The mock lane refers to untransfected cells. (B) Palmitoylation of 3×FLAG-R-Ras is not increased in the presence of a DHHG (C142G) mutant of DHHC19 in COS-7 cells. Immunodetection was carried out with a monoclonal anti-FLAG antibody. The "empty plasmid" lane corresponds to cells transfected with GFP alone. The transfection levels of wild-type DHHC19 and its C142G mutant were similar. (C) GFP-R-Ras palmitoylation decreases in the presence of five shRNAs targeted to the DHHC19 transcript in COS-7 cells by silencing the endogenous DHHC19 gene product (the shRNA templates were purchased from Sigma-Aldrich and sequences are commented in materials and methods). Note that palmitoylation is not completely abrogated, suggesting that redundant R-Ras PATs must exist in COS-7 cells. Transfection with an empty plasmid (pLKO) does not result in diminished R-Ras palmitoylation (right panel). Quantification of the immunodetection and autoradiography bands in all cases was carried out using the Fuji MultiGauge software package. The numeric values were obtained normalizing the radioactivity signal to the amount of protein as judged by the ECL signal. In all cases data are representative of at least three independent experiments.

100,000×*g* distributed almost equally into the particulate and soluble fractions. Coexpression with both the wild-type GFP-DHHC19 and the prenylation defective mutant (C279S) resulted in an increase in the percentage of membrane-associated R-Ras. Consequently, in terms of R-Ras palmitoylation, the prenylation motif in DHHC19 seems to be dispensable for activity. Likewise, the C279S DHHC19 mutant increased R-Ras palmitoylation to a similar extent as its wild-type counterpart DHHC19 (data not shown). Finally, a control was performed with compactin, diminishing the amount of prenylated R-Ras and increasing the soluble to particulate ratio of transfected R-Ras. Laser confocal microscopy revealed that YFP-R-Ras localized to the cellular plasma membrane as well as perinuclear areas of the cell (Fig. 8B). Cotransfection with CFP-DHHC19 did not significantly disturb the subcellular distribution of R-Ras. This result is consistent with R-Ras being palmitoylated by DHHC19 in Golgi areas hence modulating its plasma membrane-Golgi trafficking cycle, in analogy to the well-studied case of H-Ras [23].

We also decided to test if the increased palmitoylation of R-Ras caused by DHHC19 coexpression affected its ability to concentrate in low-fluidity subdomains of the caveolae/raft type. As shown in Fig. 8C, transfection of COS7 cells with full-length R-Ras resulted in a partial localization in fractions in which caveolin-1 was also present. Cotransfection of DHHC19 with R-Ras resulted in an increased enrichment of R-Ras in these upper (lower density) fractions, in agreement with the known localization of prenylated plus palmitoylated H-Ras proteins to these subcellular domains [24,25]. Consequently, DHHC19 is able to promote R-Ras palmitoylation resulting not only in an increased association with total cellular membranes, but specifically with membranes enriched in cholesterol/sphingomyelin that are partially resistant to Triton X-100 solubilization.

3.6. DHHC19 increases the viability of R-Ras transfected cells

R-Ras is known to increase branching morphogenesis and cell growth in murine UB cells [26] and its activated form R-Ras-G38V is known to increase significantly DNA synthesis and BrdU incorporation in Swiss 3T3 cells [27]. We tested if increased palmitoylation of R-Ras could affect its activity in a MTT viability assay of transfected NIH3T3 cells (Fig. 8D). As a control we transfected the NIH3T3 cells with a short R-Ras-GFP chimera that only included the final carboxy-terminal 11 amino acids hence lacking the GTP binding domain. As expected, wild-type R-Ras displayed a very modest increase in cell viability, although its increased palmitoylation by DHHC19 resulted in a clear increased viability. The activated form of R-Ras (V38) also positively modulated when DHHC19 was cotransfected H-Ras-V12 (a constitutively active mutant version of H-Ras) was used as a positive control of the assay and was compared to the short R-Ras version.

Finally, we decided to analyze if R-Ras and DHHC19 could be partially associated within the cell, assuming that the Golgi-associated DHHC19 might be using R-Ras as a substrate in perinuclear areas of the cell where they colocalize (Fig. 8E). When GFP-tagged DHHC19 was cotransfected with 3×FLAG-tagged R-Ras and the cell lysate was immunoprecipitated with anti-GFP antibodies a modest but reproducible quantity of R-Ras could be found in association with the palmitoyl transferase (Fig. 8E).

4. Discussion

Protein palmitoylation is a crucial post-translational modification implicated in a large number of cellular processes as diverse as protein trafficking, protein stability or lateral segregation of membrane proteins. Regulatory mechanisms have been elusive for a long time in part due to the difficulties in purifying PAT activity from cells. The breakthrough was the discovery of a protein family in yeast that displayed PAT activity [2]. Several other pertaining reports ensued [3,4,20], establishing the importance of the DHHC family of palmitoyl transferases, comprising 23 isoforms in humans. All the members of this new protein family contain a common cysteine rich domain (CRD) and a conserved aspartate-histidine-histidine-cysteine-(DHHC)-motif that also seems to be crucial for PAT activity in most cases [2,3].

In this work we analyzed the isoform DHHC19 of the DHHC family of PATs, being the only member containing a C-terminal CaaX box that is conserved among various species. This motif is a well established consensus sequence for protein prenylation, another common post-translational lipid modification. We could unequivocally show the functionality of the CaaX motif of a short chimera of DHHC19 both *in vitro* and *in vivo* (Figs. 1C and D and 2B and C) although, within our detection limits, we were unable to detect the incorporation of the radiolabelled isoprenoid moiety in full-length DHHC19. With this in mind we set out to explore the functionality of DHHC19 as a PAT.

All DHHC associated PAT activities described so far are not specific for a single substrate. In fact, in all reports that relied on *in vivo* palmitoylation assays several DHHC family members exhibited redundant PAT activity for any given substrate. There have been attempts to classify DHHC substrate fidelity *in vitro* based on the presence of certain structural motifs in the substrates, like myristoylation, isoprenylation or proximity of reactive cysteines to transmembrane regions [28], but *in vivo* data rather points at a more complex specificity pattern, likely depending on the subcellular colocalization of a given PAT and its substrate.

Many small GTPases that contain a conserved CaaX box are also palmitoylated at upstream cysteine amino acids. This dual post-translational modification has been described for H-Ras [22], N-Ras [22], K-Ras4A [11], R-Ras [12], Rap2A [14], TC10 [15], RhoB [13] and Rac1 [29] among others.

It is conceivable that a PAT with a CaaX box might be using substrates that are similarly modified at the C-terminal end, if that favours

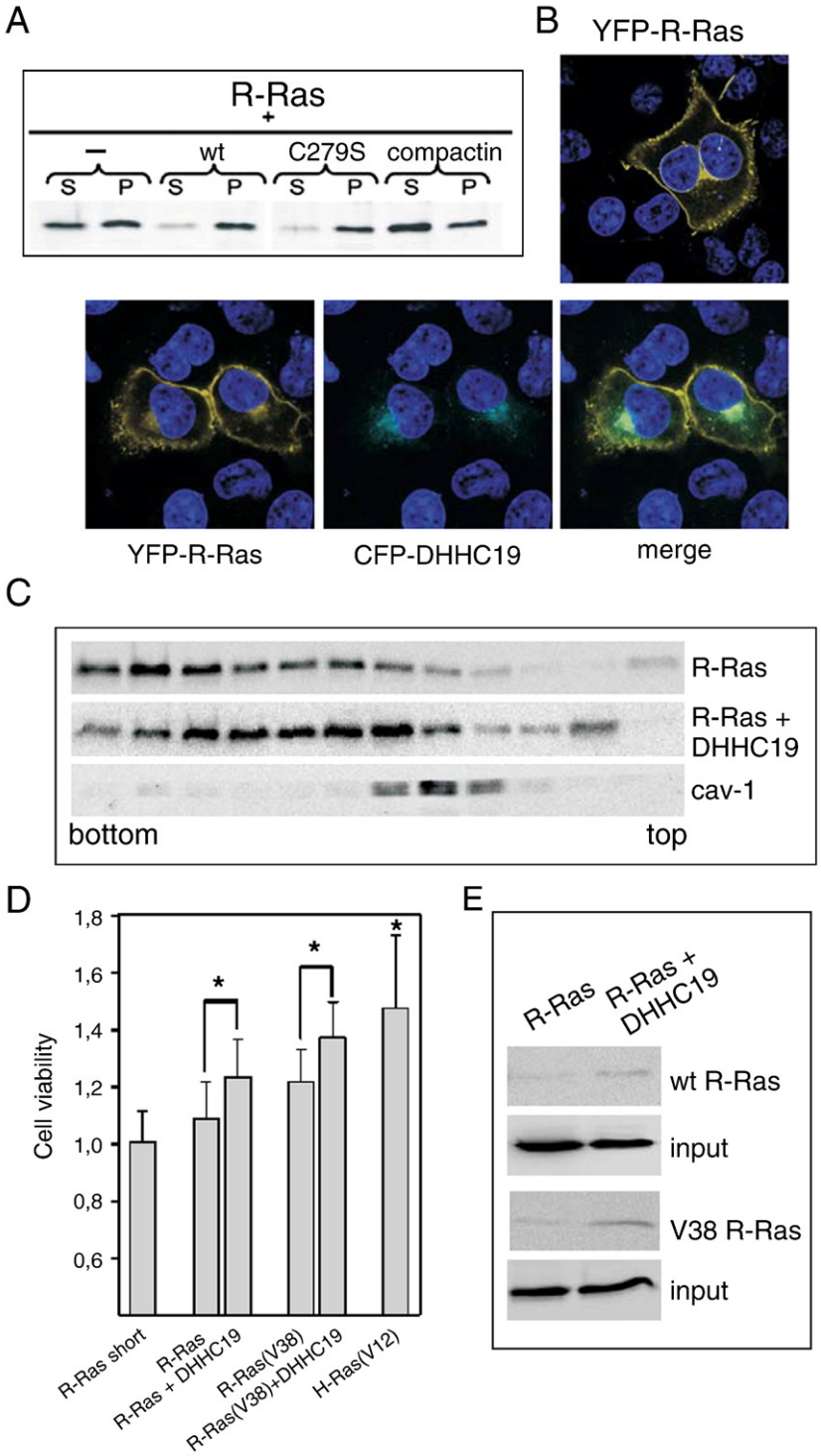

Fig. 8. DHHC19 overexpression alters the physiological function of R-Ras. (A) COS7 cells were transfected with full-length wild-type GFP-R-Ras in the absence (lanes 1–2) or presence of wild-type GFP-DHHC19 (lanes 3–4) or the mutant C279S (lanes 5–6) and the lysates were separated into supernatant and particulate fractions. As a control, a sample was also treated with a statin in order to inhibit prenyl incorporation into R-Ras (lanes 7–8). (B) YFP-R-Ras localizes to the plasma membrane and perinuclear areas of the cell (upper panel) whereas coexpression of CFP-DHHC19 and YFP-R-Ras (lower panels) does not significantly alter the latter's distribution. (C) COS7 cells were transfected with full-length wild-type GFP-R-Ras in the presence or absence of GFP-DHHC19 and the lysate was processed in a sucrose density gradient as described in the Section 2. The presence of the caveolae/rafts membrane fractions was identified using an anti-caveolin-1 antibody. Results are representative of three independent experiments. (D) NIH3T3 cells were transfected with various constructs and a MTT (3-(4,5-dimethylthiazol-2-yl)-2,5-diphenyltetrazoliumbromide) viability assay was performed. Data are expressed as mean of five independent experiments, S.D. *, $p<0.05$. In the case of H-Ras V12 *, $p<0.05$ referred to the control cells transfected with the short R-Ras construct. (E) The association of R-Ras and DHHC19 was evaluated by a co-immunoprecipitation assay. COS7 cells were transfected with constructs of a 3×FLAG-tagged wild-type and V38 mutant of R-Ras in the absence or presence of a GFP-tagged DHHC19 construct. A polyclonal anti-GFP serum was used to immunoprecipitate the GFP-tagged DHHC19 and the presence of bound R-Ras was analyzed using an anti-FLAG antibody. The "input" corresponds to an immunoblot performed on the total lysates using anti-FLAG antibodies prior to the immunoprecipitation.

colocalization of the acylating enzyme and its substrate. This hypothesis would have been in accordance with the previously reported *in vitro* data [28] suggesting the classification of substrates by structural motives. Consequently, we designed a first series of experiments, where we inspected the effect of DHHC19 on H-Ras (Fig. 5) as a representative example of the family of small GTPases that are post-translationally prenylated and palmitoylated. In principle throughout the paper, we followed the procedure proposed by Fukata et al. [30], where DHHC proteins are co-overexpressed with a putative substrate and palmitoylation is monitored by metabolic labelling, gel electrophoresis and autoradiography. Neither H-Ras or N-Ras, nor any other members of the family of small GTPases that we tested showed enhanced palmitoylation in the presence of DHHC19 with the notable exception of R-Ras (Fig. 6). Besides the modest though reproducible increase in palmitoylation of R-Ras, we could demonstrate that this effect resulted in a stronger general membrane association as judged from the enrichment in the particulate fraction (Fig. 8A) and an increase in the association of R-Ras with lipid raft/caveolae (Fig. 8C), as well as in an enhanced viability of cultured cells that had been cotransfected with both proteins (Fig. 8D). It is remarkable that this increment in R-Ras palmitoylation can have pronounced physiological effects such in the case of cell viability. This is also consistent with the amplificatory role of signalling circuits, where small changes in signalling molecules can have very profound consequences for cell fate.

In support of our data, other Ras proteins, such as H-Ras and N-Ras have previously been shown to enhance proliferation [31], tumor invasiveness and progression in a palmitoylation dependent manner. In these experiments, palmitoylation defective mutants of Ras proteins were unable to bind stably to the plasma membrane, which lead to the loss of their signalling activity. Our results indicate an increased signalling capacity of hyperpalmitoylated R-Ras that is accompanied by a stronger association to the plasma membrane and to lipid rafts/caveolae. Although the importance of lateral sorting of R-Ras has not been broadly addressed in the current literature, it has been shown that a palmitoylation defective mutant of R-Ras (C213A) was retained in the Golgi and failed to be properly transported to the plasma membrane, while wild-type R-Ras has been shown to effectively exit the Golgi and to be predominantly located in focal adhesions [32]. This effect is comparable to other Ras proteins, where the lack of palmitoylation results in Golgi accumulation [33]. Furthermore, R-Ras function has been shown to be involved in integrin signalling, probably from focal adhesions, and to involve different signalling routes than the classical Ras proteins. Taking into account all this evidence, it is feasible that there exists a specific PAT for R-Ras that does not interfere with the other Ras isoforms that activate different signalling routes in the cell.

Finally, we correlate an increased association of R-Ras with lipid rafts/caveolae-like domains with an increase in physiological activity, as judged from enhanced viability of transformed cells. The correlation would be supported by the fact that N-Ras in its GTP loaded (active) state depended on cholesterol-sensitive micro domains for its clustering [25]. R-Ras is also monopalmitoylated like N-Ras (and unlike dipalmitoylated H-Ras). Hence, hyperpalmitoylation of R-Ras by DHHC19 could increase its partition into lipid raft/caveolae-like domains and enhance its activity. We could observe this effect both towards wild-type R-Ras and towards its constitutively GTP loaded version (R-Ras-G38V). Therefore, hyperpalmitoylation seems to affect both R-Ras pools in a similar way.

Interestingly, we were unable to reproduce the previously reported *in vitro* data where H-Ras was shown to be palmitoylated by recombinantly expressed DHHC9 and its co-factor GCP16. GCP16 is ubiquitously expressed and DHHC9 was shown to be expressed in several tissues as well [21]. However, overexpression of DHHC9 in COS7 cells together with GFP-tagged H-Ras did not result in an increased palmitoylation in our hands. Consequently, *in vitro* palmitoylation data might not exactly reflect the *in vivo* situation where the subcellular localization of DHHC proteins relative to their potential substrates dictates substrate specificity.

Subcellular localization studies of DHHC19 revealed that it is mainly located to trans-Golgi regions as judged by the colocalization with the trans-Golgi markers TGN38 and Gal-T (Fig. 3). Interestingly, R-Ras like other Ras isoforms also localizes to Golgi regions, while displaying some plasma membrane localization as well. Rocks et al. showed that a palmitoylation/depalmitoylation dependent process redistributes H-Ras between Golgi and plasma membrane [23]. It would be intriguing if R-Ras localization was controlled by a similar mechanism, where its palmitoylation depended on DHHC19 in the Golgi. This possibility, however, has yet to be established.

Northern Blot analysis showed that DHHC19 is specifically expressed in lung, testis, thymus and small intestine [21] whereas R-Ras is expressed in all tissues tested [34]. Therefore, DHHC19 might be responsible for the modulation of R-Ras in tissues in which both proteins concur while other DHHC proteins might be responsible for the modulation of R-Ras palmitoylation in other tissues in which DHHC19 is not expressed. Notably, it has been shown that R-Ras is specifically modulated in testis and brain by a Ras-Guanine Nucleotide releasing factor (Ras-GRF) that is expressed only in these tissues [34]. It is possible that in the case of DHHC-dependent palmitoylation the expression patterns of DHHC proteins define their cognate substrates and hence their modulation. In this work, R-Ras palmitoylation was monitored in COS7 cells (green monkey kidney cells). We could observe endogenous palmitoylation of R-Ras in COS7 cells (just as with other substrates, such as SNAP25 or RhoB for instance). Considering the results obtained with the DHHC19 shRNAs, we could conclude that these cells must express DHHC19 together with other PATs that can also use R-Ras as a substrate. Others have reported that DHHC protein specificity can depend on inherent protein binding domains like ankyrin repeats, like in the case of DHHC17 (HIP14) [4,35]. On the other hand, specificity also seems to be conferred by the expression pattern in distinct micro environments of the cell. It will surely be of interest in the future to address more in detail the question of how the DHHC family of PATs achieves substrate specificity *in vivo*.

Finally, while we could show that DHHC19 contains a putative prenylation motif at the C-terminal end, it did not seem to be of importance for DHHC19 mediated R-Ras modulation (Fig. 8A). In fact, both the wild-type and the mutant with the altered CaaX box equally promote R-Ras palmitoylation and its increased association with membranes. Possibly, isoprenylation of DHHC19 is not essential for its effect on R-Ras in general, but for a more subtle fine tuning of its activity. With our methodology, we only capture average steady state palmitoylation and its effects on target proteins. It is conceivable that isoprenylation of DHHC19 has some effect on the time course of the palmitoylation of certain substrates. On the other hand, it has been reported that isoprenylation of the SNARE protein Ykt6 increases its stability [36]. Furthermore, isoprenylation of H-Ras has previously been shown to be necessary for the interaction with its co-factors [37] and not solely for membrane tethering. Hence, isoprenylation can have diverse functions both in membrane and in soluble proteins that go beyond a mere membrane anchor. The isoprenylation of DHHC19 could therefore be responsible for the fine tuning of its micro localization in the cell, for its stability or for the interaction with co-factors or substrates. As a matter of fact, isoprenylation is not important for the effects on R-Ras that we addressed, but its importance might lie in aspects that more detailed studies will bring to light.

Acknowledgements

We would like to thank Dr. Francisco Gavilanes-Franco for his kind help with the HPLC experiments. We are also indebted to Dr. Dolores Pérez-Sala for providing us with materials and advice. This research was in part funded by a Marie Curie EST fellowship from the European Union. This research was funded by grants from the Spanish

Ministerio de Ciencia e Innovación BIO2009-09694 and BFU2009-10442.

References

[1] D.J. Bartels, D.A. Mitchell, X. Dong, R.J. Deschenes, Erf2, a novel gene product that affects the localization and palmitoylation of Ras2 in *Saccharomyces cerevisiae*, Mol. Cell. Biol. 19 (1999) 6775–6787.

[2] S. Lobo, W.K. Greentree, M.E. Linder, R.J. Deschenes, Identification of a Ras palmitoyltransferase in *Saccharomyces cerevisiae*, J. Biol. Chem. 277 (2002) 41268–41273.

[3] M. Fukata, Y. Fukata, H. Adesnik, R.A. Nicoll, D.S. Bredt, Identification of PSD-95 palmitoylating enzymes, Neuron 44 (2004) 987–996.

[4] K. Huang, et al., Huntingtin-interacting protein HIP14 is a palmitoyl transferase involved in palmitoylation and trafficking of multiple neuronal proteins, Neuron 44 (2004) 977–986.

[5] C. Fernandez-Hernando, M. Fukata, P.N. Bernatchez, Y. Fukata, M.I. Lin, D.S. Bredt, W.C. Sessa, Identification of Golgi-localized acyl transferases that palmitoylate and regulate endothelial nitric oxide synthase, J. Cell Biol. 174 (2006) 369–377.

[6] J. Greaves, C. Salaun, Y. Fukata, M. Fukata, L.H. Chamberlain, Palmitoylation and membrane interactions of the neuroprotective chaperone cysteine-string protein, J. Biol. Chem. 283 (2008) 25014–25026.

[7] R. Tsutsumi, Y. Fukata, J. Noritake, T. Iwanaga, F. Perez, M. Fukata, Identification of G protein alpha subunit-palmitoylating enzyme, Mol. Cell. Biol. 29 (2009) 435–447.

[8] C.A. Keller, X. Yuan, P. Panzanelli, M.L. Martin, M. Alldred, M. Sassoe-Pognetto, B. Luscher, The gamma2 subunit of GABA(A) receptors is a substrate for palmitoylation by GODZ, J. Neurosci. 24 (2004) 5881–5891.

[9] J. Zhang, S.L. Planey, C. Ceballos, S.M. Stevens Jr., S.K. Keay, D.A. Zacharias, Identification of CKAP4/p63 as a major substrate of the palmitoyl acyltransferase DHHC2, a putative tumor suppressor, using a novel proteomics method, Mol. Cell. Proteomics 7 (2008) 1378–1388.

[10] C. Sharma, X.H. Yang, M.E. Hemler, DHHC2 affects palmitoylation, stability, and functions of tetraspanins CD9 and CD151, Mol. Biol. Cell 19 (2008) 3415–3425.

[11] J.E. Buss, B.M. Sefton, Direct identification of palmitic acid as the lipid attached to p21ras, Mol. Cell. Biol. 6 (1986) 116–122.

[12] D.G. Lowe, D.V. Goeddel, Heterologous expression and characterization of the human R-ras gene product, Mol. Cell. Biol. 7 (1987) 2845–2856.

[13] P. Adamson, C.J. Marshall, A. Hall, P.A. Tilbrook, Post-translational modifications of p21rho proteins, J. Biol. Chem. 267 (1992) 20033–20038.

[14] F. Beranger, A. Tavitian, J. de Gunzburg, Post-translational processing and subcellular localization of the Ras-related Rap2 protein, Oncogene 6 (1991) 1835–1842.

[15] D. Michaelson, J. Silletti, G. Murphy, P. D'Eustachio, M. Rush, M.R. Philips, Differential localization of Rho GTPases in live cells: regulation by hypervariable regions and RhoGDI binding, J. Cell Biol. 152 (2001) 111–126.

[16] A. Kalinin, N.H. Thoma, A. Iakovenko, I. Heinemann, E. Rostkova, A.T. Constantinescu, K. Alexandrov, Expression of mammalian geranylgeranyltransferase type-II in *Escherichia coli* and its application for in vitro prenylation of Rab proteins, Protein Expr. Purif. 22 (2001) 84–91.

[17] M.P. Lisanti, M. Sargiacomo, P.E. Scherer, Purification of caveolae-derived membrane microdomains containing lipid-anchored signaling molecules, such as GPI-anchored proteins, H-Ras, Src-family tyrosine kinases, eNOS, and G-protein alpha-, beta-, and gamma-subunits, Methods Mol. Biol. 116 (1999) 51–60.

[18] I. Navarro-Lerida, A. Alvarez-Barrientos, F. Gavilanes, I. Rodriguez-Crespo, Distance-dependent cellular palmitoylation of de-novo-designed sequences and their translocation to plasma membrane subdomains, J. Cell Sci. 115 (2002) 3119–3130.

[19] T. Mosmann, Rapid colorimetric assay for cellular growth and survival: application to proliferation and cytotoxicity assays, J. Immunol. Methods 65 (1983) 55–63.

[20] J.T. Swarthout, S. Lobo, L. Farh, M.R. Croke, W.K. Greentree, R.J. Deschenes, M.E. Linder, DHHC9 and GCP16 constitute a human protein fatty acyltransferase with specificity for H- and N-Ras, J. Biol. Chem. 280 (2005) 31141–31148.

[21] Y. Ohno, A. Kihara, T. Sano, Y. Igarashi, Intracellular localization and tissue-specific distribution of human and yeast DHHC cysteine-rich domain-containing proteins, Biochim. Biophys. Acta 1761 (2006) 474–483.

[22] J.F. Hancock, A.I. Magee, J.E. Childs, C.J. Marshall, All ras proteins are polyisoprenylated but only some are palmitoylated, Cell 57 (1989) 1167–1177.

[23] O. Rocks, et al., An acylation cycle regulates localization and activity of palmitoylated Ras isoforms, Science 307 (2005) 1746–1752.

[24] B. Rotblat, I.A. Prior, C. Muncke, R.G. Parton, Y. Kloog, Y.I. Henis, J.F. Hancock, Three separable domains regulate GTP-dependent association of H-ras with the plasma membrane, Mol. Cell. Biol. 24 (2004) 6799–6810.

[25] S. Roy, et al., Individual palmitoyl residues serve distinct roles in H-ras trafficking, microlocalization, and signaling, Mol. Cell. Biol. 25 (2005) 6722–6733.

[26] A. Pozzi, et al., H-Ras, R-Ras, and TC21 differentially regulate ureteric bud cell branching morphogenesis, Mol. Biol. Cell 17 (2006) 2046–2056.

[27] A.J. Self, E. Caron, H.F. Paterson, A. Hall, Analysis of R-Ras signalling pathways, J. Cell Sci. 114 (2001) 1357–1366.

[28] A.S. Varner, C.E. Ducker, Z. Xia, Y. Zhuang, M.L. De Vos, C.D. Smith, Characterization of human palmitoyl-acyl transferase activity using peptides that mimic distinct palmitoylation motifs, Biochem. J. 373 (2003) 91–99.

[29] R. Kang, et al., Neural palmitoyl-proteomics reveals dynamic synaptic palmitoylation, Nature 456 (2008) 904–909.

[30] Y. Fukata, T. Iwanaga, M. Fukata, Systematic screening for palmitoyl transferase activity of the DHHC protein family in mammalian cells, Methods 40 (2006) 177–182.

[31] T. Dudler, M.H. Gelb, Palmitoylation of Ha-Ras facilitates membrane binding, activation of downstream effectors, and meiotic maturation in *Xenopus oocytes*, J. Biol. Chem. 271 (1996) 11541–11547.

[32] J. Furuhjelm, J. Peranen, The C-terminal end of R-Ras contains a focal adhesion targeting signal, J. Cell Sci. 116 (2003) 3729–3738.

[33] E. Choy, V.K. Chiu, J. Silletti, M. Feoktistov, T. Morimoto, D. Michaelson, I.E. Ivanov, M.R. Philips, Endomembrane trafficking of ras: the CAAX motif targets proteins to the ER and Golgi, Cell 98 (1999) 69–80.

[34] T. Gotoh, Y. Niino, M. Tokuda, O. Hatase, S. Nakamura, M. Matsuda, S. Hattori, Activation of R-Ras by Ras-guanine nucleotide-releasing factor, J. Biol. Chem. 272 (1997) 18602–18607.

[35] K. Huang, R. Singaraja, F. Young, N. Davis, M. Hayden, A. El-Husseini, Palmitoyl transferase specificity towards huntingtin and other neuronal proteins. In Neuroscience Meeting ed.^eds), San Diego (2007).

[36] O. Pylypenko, A. Schonichen, D. Ludwig, C. Ungermann, R.S. Goody, A. Rak, M. Geyer, Farnesylation of the SNARE protein Ykt6 increases its stability and helical folding, J. Mol. Biol. 377 (2008) 1334–1345.

[37] K.A. Cadwallader, H. Paterson, S.G. Macdonald, J.F. Hancock, N-terminally myristoylated Ras proteins require palmitoylation or a polybasic domain for plasma membrane localization, Mol. Cell. Biol. 14 (1994) 4722–4730.

[38] P.J. Roberts, et al., Rho family GTPase modification and dependence on CAAX motif-signaled posttranslational modification, J. Biol. Chem. 283 (2008) 25150–25163.